R-spondin 2 promotes osteoblastic differentiation of immature human periodontal ligament cells through the Wnt/beta-catenin signaling pathway

Arima, Mai
Department of Endodontology and Operative Dentistry, Faculty of Dental Science, Kyushu University

Hasegawa, Daigaku
Division of Endodontology, Kyushu University Hospital, Kyushu University

Yoshida, Shinichiro
Division of Endodontology, Kyushu University Hospital, Kyushu University

Mitarai, Hiromi
Division of General Dentistry, Kyushu University Hospital, Kyushu University

他

出版情報：Journal of Periodontal Research. 154 (2), pp.143-153, 2018-10-04. Munksgaard International Publishers
バージョン：
権利関係：

R-spondin 2 promotes osteoblastic differentiation of immature human periodontal ligament cells through the Wnt/β-catenin signaling pathway

M. Arima[1], D. Hasegawa[2], S. Yoshida[2], H. Mitarai[3], A. Tomokiyo[2], S. Hamano[1,4], H. Sugii[2], N. Wada[3], H. Maeda[1,2]

[1]Department of Endodontology and Operative Dentistry, Faculty of Dental Science, Kyushu University, Fukuoka, Japan

[2]Division of Endodontology, Kyushu University Hospital, Kyushu University, Fukuoka, Japan

[3] Division of General Dentistry, Kyushu University Hospital, Kyushu University, Fukuoka, Japan

[4] Faculty of Dental Science, OBT Research Center, Kyushu University, Fukuoka, Japan

Correspondence:

Hidefumi Maeda

Department of Endodontology and Operative Dentistry,

Faculty of Dental Science,

Kyushu University,

3-1-1 Maidashi,

Fukuoka 812-8582,

Japan,

Fax: +81 92 642 6366.

E-mail address: hide@dent.kyushu-u.ac.jp (H. Maeda).

Funding information:

JSPS KAKENHI grant numbers JP15H05023, JP16K20457, JP16K20458, JP17H01598, and JP17H04385

Key words: Periodontal ligament, Osteoblastic differentiation, R-spondin 2, Wnt/β-catenin signaling pathway

Abstract

Objective

In this study, we measured the expression of R-spondin 2 (RSPO2) in periodontal ligament (PDL) tissue and cells. Further, we examined the effects of RSPO2 on osteoblastic differentiation of immature human PDL cells (HPDLCs).

Background

R-spondin (RSPO) family proteins are secreted glycoproteins that play important roles in embryonic development and tissue homeostasis through activation of the Wnt/β-catenin signaling pathway. RSPO2, a member of the RSPO family, has been reported to enhance osteogenesis in mice. However, little is known regarding the roles of RSPO2 in PDL tissues.

Methods

Expression of RSPO2 in rat PDL tissue and primary HPDLCs was examined by immunohistochemical and immunofluorescence staining, as well as by semi-quantitative RT-PCR. The effects of stretch loading on the expression of RSPO2 and Dickkopf-related protein 1 (DKK1) were assessed by quantitative RT-PCR. Expression of receptors for RSPOs, such as *Leucine-rich repeat-containing G-protein coupled receptors (LGRs) 4, 5,* and *6* in immature human PDL cells (cell line 2-14, or 2-14 cells) was investigated by

semi-quantitative RT-PCR. Mineralized nodule formation in 2-14 cells treated with RSPO2 under osteoblastic inductive condition was examined by Alizarin Red S and von Kossa stainings. Nuclear translocation of β-catenin and expression of active β-catenin in 2-14 cells treated with RSPO2 were assessed by immunofluorescence staining and western blotting analysis, respectively. In addition, the effect of Dickkopf-related protein 1 (DKK1), an inhibitor of Wnt/β-catenin signaling, was also examined.

Results

Rat PDL tissue and HPDLCs expressed RSPO2, and HPDLCs also expressed *RSPO2*, while little was found in 2-14 cells. Expression of *RSPO2* as well as *DKK1* in HPDLCs was significantly upregulated by exposure to stretch loading. *LGR4* was predominantly expressed in 2-14 cells, which expressed low levels of *LGR5* and *LGR6*. RSPO2 enhanced the Alizarin Red S and von Kossa-positive reactions in 2-14 cells. In addition, DKK1 suppressed nuclear translocation of β-catenin, activation of β-catenin, and increases of Alizarin Red S and von Kossa positive reactions in 2-14 cells, all of which were induced by RSPO2 treatment.

Conclusion

RSPO2, which is expressed in PDL tissue and cells, might play an important role in regulating the osteoblastic differentiation of immature human PDL cells through the

Wnt/β-catenin signaling pathway.

1 Introduction

Periodontal tissue comprises periodontal ligament (PDL), alveolar bone, cementum, and gingiva. The functions of PDL include tooth support, homeostasis, and repair of damaged periodontal tissue[1-3]. Moreover, PDL tissue constitutively undergoes mechanical stress, such as occlusion and mastication[4], and maintains structural integrity by adjusting cell functions under this condition[5]. However, PDL tissue experiences difficulty in regeneration after severe damage from disease-related inflammation (i.e., caused by periodontitis or deep caries). Thus, many studies have explored methods to facilitate PDL tissue regeneration through tissue engineering techniques, employing effective stem cells, signaling molecules, and scaffolds.

The PDL cell population consists of various cell types, including fibroblasts (the major cells in PDL[6]), osteoblasts, cementoblasts, epithelial cell rests of Malassez, and PDL stem/progenitor cells. PDL stem cells are reported to differentiate into both collagen fiber-forming cells and mineralized tissue-forming cells, such as osteoblasts and cementoblasts[7]. Therefore, immature PDL cells are responsible for PDL tissue healing and repair, as well as structural preservation.

In our previous study, we succeeded in immortalizing human PDL cells (HPDLCs) by transfection of the cells with Simian virus 40 large T-antigen and human telomerase

reverse transcriptase. These cells were confirmed to preserve the properties of primary PDL cells[8]. Furthermore, we established and characterized clonal human PDL stem cell lines from these immortalized cells[9, 10]. In the present study, we examined the stemness of another cell line, 2-14 ("2-14 cells"), and characterized the effects of R-spondin 2 (RSPO2) on the osteoblastic differentiation of this cell line.

R-spondin (RSPO) family proteins comprise a four-member family of secreted glycoproteins, RSPO1-4. Several studies have reported that RSPO proteins activate the Wnt/β-catenin signaling pathway by interaction with Frizzled 8 and low-density-lipoprotein-receptor-related proteins 5 and 6[11]. Recent studies have shown that receptors for RSPOs comprise leucine-rich-repeat-containing G-protein-coupled receptors 4, 5, and 6 (LGR4, LGR5, and LGR6)[12, 13]. RSPO2 plays essential roles in various biological processes, including skeletal development; notably, Rspo2-knockout mice showed facial skeletal defects, distal limb loss, and lung hypoplasia, and these mice died immediately after birth[14]. Additionally, previous studies have shown that RSPO2 promotes osteogenesis by activating the Wnt/β-catenin signaling pathway in MC3T3-E1 cells[15]. However, the role of RSPO2 in PDL tissue remains unclear. Therefore, we hypothesized that RSPO2 might promote osteogenesis in immature PDL cells by activating the Wnt/β-catenin signaling pathway. In this study, we examined the expression of RSPO2 in PDL

tissue and HPDLCs, and characterized the effects of RSPO2 and its related signaling on the osteoblastic differentiation of immature human PDL cells.

2 Material and Methods

2.1 Reagents

Recombinant human RSPO2 (rhRSPO2), Dickkopf1 (rhDKK1), and TGF-β3 (rhTGF-β3) were purchased from R&D Systems (Minneapolis, MN, USA).

2.2 Cell culture

Three HPDLC cultures were isolated from the healthy wisdom tooth of a 22-year-old female (HPDLC-3D), a 23-year-old male (HPDLC-3S), and a 25-year-old female (HPDLC-3U) with informed consent, as described previously[16]. A clonal cell line, 2-14, was isolated from immortalized human PDL cells, which were established in our previous study[8]. HPDLCs, from passages four through six, and 2-14 cells were maintained in alpha minimum essential medium (αMEM; Gibco-BRL, Grand Island, NY, USA) containing 10% fetal bovine serum (FBS; Biosera, Nuaillé, France; 10% FBS/αMEM) at 37°C in a humidified atmosphere of 5% CO_2 and 95% air. All procedures were performed in compliance with requirements of the Research Ethics Committee at Kyushu University.

2.3 Immunohistochemical staining

Five-week-old male Sprague-Dawley (SD) rats (Kyudo, Saga, Japan) were perfused

transcardially with 4% paraformaldehyde (PFA; Merck Millipore, Darmstadt, Germany) in phosphate-buffered saline (PBS) under anesthesia. The jaws were excised and immersed in 4% PFA for an additional 24 h. The tissues were then washed with PBS and decalcified in 10% ethylenediaminetetraacetic acid for 4 w at 4°C before dehydration and embedding in paraffin. The embedded tissues were sectioned (5 µm thick); these sections were deparaffinized, and non-specific antigens were blocked with 2% bovine serum albumin (BSA; Nacalai Tesque, Kyoto, Japan) for 1 h at room temperature (RT). A goat polyclonal anti-RSPO2 antibody (1:50 dilution; Santa Cruz Biotechnology, Santa Cruz, CA, USA) and a rabbit monoclonal anti-DKK1 antibody (1:100 dilution; Abcam, Cambridge, UK) were applied as the primary antibody, overnight at 4°C. Sections were then incubated with biotinylated anti-goat IgG (Nichirei Biosciences, Inc., Tokyo, Japan) or biotinylated anti-rabbit IgG (Nichirei) as the secondary antibody at RT for 30 min, followed by an avidin-peroxidase conjugate (Nichirei) for 30 min at RT. Positive staining was visualized using Simple Stain DAB solution (Nichirei). Staining of nuclei was performed using Mayer's hematoxylin solution (Wako Pure Chemical Industries Ltd., Osaka, Japan). All procedures were approved by the Animal Ethics Committee and conformed to the regulations of Kyushu University.

2.4 Immunofluorescence staining

HPDLCs and 2-14 cells were fixed with 4% PFA (Merck Millipore) and 0.5% dimethyl sulfoxide (Wako) in PBS for 20 min at RT. After being blocked with 2% BSA in PBS for 1 h at RT, the cells were incubated with a goat polyclonal anti-RSPO2 antibody (1:50 dilution; Santa Cruz), a rabbit polyclonal anti-LGR4 antibody (1:100 dilution; Abcam, Cambridge, UK), or a rabbit monoclonal anti-β-catenin antibody (1:100 dilution; Cell Signaling Technology, Beverly, MA, USA), as the primary antibody, overnight at 4°C. The cells were then incubated with an Alexa 568-conjugated donkey anti-goat IgG secondary antibody (1:200 dilution; Invitrogen, Carlsbad, CA, USA) or an Alexa 488-conjugated chicken anti-rabbit IgG secondary antibody (1:200 dilution; Invitrogen) for 30 min at RT. The cells were then washed with PBS and counterstained with 4',6-diamidino-2-phenylindole (DAPI; Vector Laboratories, Burlingame, CA, USA). The cells were imaged and analyzed using a Biozero digital microscope (Keyence, Osaka, Japan).

2.5 Semi-quantitative RT-PCR

Total cellular RNA was isolated with TRIzol Reagent (Invitrogen), in accordance with the manufacturer's instructions. First-strand cDNA was synthesized from 1 mg total RNA by using an ExScript RT Reagent kit (Takara Bio Inc., Shiga, Japan). Total RNA was

reverse-transcribed with random 6-mers and ExScript RTase for 15 min at 42°C; the reaction was stopped by incubation for 2 min at 99°C, followed by 5 min at 5°C. PCR was performed using Platinum Taq DNA polymerase (Invitrogen) in a PCR Thermal Cycler Dice (Takara) under the following conditions: 94°C for 2 min, then the appropriate number of cycles at [94°C for 30 s; appropriate annealing temperature for 30 s; 72°C for 30 s], and finally 72°C for 7 min, in accordance with our recent study[17]. Primer sequences, annealing temperatures, cycle number, and product sizes for *RSPO2*, *LGR4*, *LGR5*, *LGR6*, and *glyceraldehyde3-phosphate dehydrogenase (GAPDH)* are shown in Table 1. *GAPDH* primers were used as internal standards. All PCR assays were performed within the exponential amplification range. PCR products were separated by electrophoresis on 2% agarose gels (Seakem ME; BioWhittaker Molecular Applications, Rockland, ME, USA) and photographed under ultraviolet excitation after ethidium bromide staining.

2.6 Quantitative RT-PCR

PCR was performed using KAPA Express Extract (Kapa Biosystems, Woburn, MA, USA) in a Thermal Cycler Dice Real Time System (Takara) under the following conditions: 95°C for 10 s (initial denaturation), then 40 cycles at 95°C for 5 s and 60°C for 30 s, followed by a dissociation protocol at 95°C for 15 s, 60°C for 30 s, and 95°C for 15 s, in

accordance with our recent study[18]. Primer sequences, annealing temperatures, cycle numbers, and product sizes for *DKK1*, *RSPO2*, *CD49d*, *CD146, N-cadhelin*, *p75NTR,* and *β-actin* are shown in Table 2. *β-actin* was used as an internal standard. Expression levels of target genes were calculated using ΔΔCt values.

2.7 Application of stretch loading

HPDLCs were pre-cultured in flexible-bottomed culture chambers (STREX Co., Osaka, Japan) coated with type-I collagen (Cell matrix I-P, Nitta Gelatin Inc., Osaka, Japan) until reaching sub-confluence, as recently described[19]. Subsequently, stretch loading was applied to HPDLC cultures with a STB-140 (STREX Co.), which uni-axially stretched culture chambers at 37°C in a humidified atmosphere of 5% CO_2 and 95% air. The force conditions were 0.5 Hz (30 cycles/min) with 10% elongation for 24 h. This force represented the physiological conditions of occlusal force[20]. After stretch loading, HPDLCs underwent RNA extraction. Cells seeded on the chambers without stretching served as controls.

2.8 Osteoblastic differentiation assay

Culture medium with 2 mM $CaCl_2$ was used as the osteoblastic induction medium, in

accordance with our previous study[21]. Briefly, 2-14 cells (1×10^4 cells/well) were seeded on 24-well plates (Becton Dickinson) in four different media: 10% FBS/αMEM as control culture medium; 10% FBS/αMEM containing 2 mM $CaCl_2$; 10% FBS/αMEM containing both 2 mM $CaCl_2$ and 100 ng/ml rhRSPO2; and 10% FBS/αMEM containing 2 mM $CaCl_2$, 100 ng/ml rhRSPO2, and 100 ng/ml rhDKK1. After 20 days of culture, the cells were subjected to Alizarin Red S and von Kossa stainings. The area of each Alizarin Red-positive region was measured using a Biozero digital microscope (Keyence).

2.9 Adipogenic differentiation assay

2-14 cells (1×10^4 cells/well) were seeded on 48-well plates in 10% FBS/αMEM in the presence of 0.5 mM methylisobutylmethylxabthine (Sigma, St. Louis, MO, USA), 0.5 μM hydrocortisone (Sigma), 60 μM indomethacin (Sigma), and 100 μM ascorbic acid (Nacalai) for 4 w, as previously described[22]. Lipid-containing fat cells were identified by Oil-Red O staining.

2.10 Chondrogenic differentiation assay

Suspensions of 2-14 cells (2.5×10^5 cells/tube) in 15 ml polypropylene tubes (Thermo Fisher Scientific, Waltham, MA, USA) were centrifuged at 150 g for 5 min, then cultivated

in presence of chondrogenic medium with 10 ng/ml rhTGF-β3 (R&D Systems) for 4 w, as previously described[10]. After undergoing fixation with 4% PFA in PBS, the pellets were embedded in paraffin and sectioned in 5-μm thick slices. Alcian blue staining was performed to identify cartilaginous matrix.

2.11 Flow cytometric analysis

The expression of cell surface antigens in 2-14 cells was analyzed by flow cytometry. 2-14 cells (2×10^5 cells/tube), prepared as single cell suspension by trypsin/EDTA digestion and resuspension in flow cytometry buffer (R&D Systems), were incubated with antibodies (10 mg/ml) specific for surface markers or isotype control antibodies (10 mg/ml) on ice for 45 min. Antibodies reactive to CD29-PE, CD44-PE, CD90-PE, CD105-PE, CD146-PE (eBioscience, San Diego, CA, USA), and mouse IgG isotype control-PE, were used. The cells were washed with flow cytometry staining buffer and analyzed using an EC800 cell analyzer (Sony Biotechnology, Tokyo, Japan).

2.12 Western blotting analysis

2-14 cells, cultured in 10% FBS/αMEM, were treated with 2 mM $CaCl_2$, 100 ng/ml rhRSPO2, and 100 ng/ml rhDKK1 for 24 h. The cells were lysed in a buffer containing

50 mM TRIS-HCl, pH 6.9 (Sigma), 2% sodium dodecylsulfate (SDS; Nacalai), 6% 2-mercaptoethanol (Sigma), and 10% glycerol. Aliquots containing 10 mg protein/lane were subjected to 4–20% SDS polyacrylamide gel electrophoresis, then transferred onto an Immuno-Blot PVDF membrane (Bio-Rad Laboratories, Hercules, CA, USA). The membrane was reacted with mouse monoclonal anti-β-actin (Santa Cruz) at a dilution of 1:1000, rabbit monoclonal anti-β-catenin antibody (Cell Signaling) at a dilution of 1:100, or rabbit monoclonal anti-non-phospho (active) β-catenin (Ser33/37/Thr41) (D13A1) (Cell Signaling) at a dilution of 1:100, respectively. The reactions were followed by incubation with biotinylated anti-mouse IgG (Nichirei) or anti-rabbit IgG (Nichirei). After the membrane was washed thoroughly, the reactive bands were visualized using ECL prime western blotting detection system (GE Healthcare, Buckinghamshire, UK). Full-Range Rainbow Molecular Weight Markers (GE Healthcare) and BLUeye Prestained Protein Ladder (GeneDireX Inc., Las Vegas, NV, USA) were used as standard protein ladders.

2.13 Statistical analysis

All experiments were performed in triplicate or quadruplicate. All values are expressed as the mean ± standard deviation (SD). Statistical analysis was performed using

Student's unpaired t-test for comparisons of two groups and one-way ANOVA followed by the Benjamini-Hochberg method for comparisons of three or more groups. $P<0.05$ was considered statistically significant.

3 Results

3.1 Expression of RSPO2 in PDL tissues and cells

Immunohistochemical staining revealed positive staining with anti-RSPO2 antibody in rat PDL tissue, while faint positive staining was observed in dental pulp tissue **(Fig. 1A, B)**. In addition, osteocytes showed negative reaction **(Fig. 1C)**. Control staining was negative in PDL tissue **(Fig. 1D)**.

Semi-quantitative RT-PCR analysis revealed clear expression of *RSPO2* in three HPDLCs, but little expression in 2-14 cells **(Fig. 1E)**. Immunofluorescence analysis also showed intense staining for RSPO2 in HPDLCs, but exhibited faint reaction in 2-14 cells **(Fig. 1F-I)**. The results were almost the same as those of RT-PCR. Control staining was negative **(Fig. 1J-M)**.

3.2 Effects of stretch loading on RSPO2 and DKK1, and expression of DKK1 in HPDLCs

We applied stretch loading to HPDLCs with 10% elongation (0.5 Hz) for 24 h and assessed the gene expression of *RSPO2* and *DKK1* by quantitative RT-PCR. The gene expressions of *RSPO2* and *DKK1* in HPDLCs was significantly upregulated by exposure to stretch loading, compared with non-loaded cells **(Fig. 2A-F)**. Immunohistochemical

staining also exhibited positive reaction for anti-DKK1 antibody in rat PDL tissue **(Fig. 2G)**. Control staining was negative in PDL tissue **(Fig. 2H)**.

3.3 Characterization of cell line 2-14 ("2-14 cells")

In this study, we decided to develop and use a clonal undifferentiated human PDL cell line, 2-14 cells, to investigate the effects of RSPO2 on the osteoblastic differentiation of immature PDL cells because PDL cells consists of heterogeneous cell populations and very few number of PDL stem cells is included. This cell line exhibited a spindle-like shape **(Fig. 3A)**. First, to analyze the stem cell features of this cell line, we examined its differentiation potential. The cells were subjected to osteoblastic, adipogenic, and chondrogenic inductions *in vitro*. After osteoblastic induction, 2-14 cells formed Alizarin Red S-positive calcified deposits **(Fig. 3B)**. 2-14 cells cultured under adipogenic conditions produced numerous Oil Red O-positive lipid vacuoles **(Fig. 3C)**. Under chondrogenic conditions, pellet-cultured 2-14 cells synthesized alcian blue-positive cartilaginous matrix **(Fig. 3D)**. Quantitative RT-PCR demonstrated increased expression of stem cell-related genes, such as *CD49d*, *CD146*, *N-cadhelin*, and *p75NTR* in 2-14 cells, compared with HPDLCs **(Fig. 3E)**. Moreover, 2-14 cells were found to express MSC-related markers, such as CD29, CD44, CD90, CD105, and CD146, by flow

cytometric analysis **(Fig. 3F)**. These results indicated that 2-14 cells possess characteristics of human PDL stem/progenitor cells.

3.4 Expression of receptors of RSPO2 in 2-14 cells and the effects of RSPO2 on osteoblastic differentiation of 2-14 cells

First, 2-14 cells were examined for the expression of receptors of RSPO2 by semi-quantitative RT-PCR. The results showed that this cell line clearly expressed LGR4, but little expressed LGR5 and LGR6 **(Fig. 4A)**. In addition, the expression of LGR4 was evident by immunofluorescence staining **(Fig. 4B, C)**. Next, 2-14 cells were cultured in osteoblastic differentiation medium, with or without 100 ng/ml RSPO2. After 20 days of culture, RSPO2 stimulation led to enhanced Alizarin Red S and von Kossa-positive areas, compared with the $CaCl_2$-treated group **(Fig. 4D, E)**.

3.5 Effects of DKK1 on RSPO2-induced acceleration of osteoblastic differentiation of 2-14 cells

The nuclear translocation of β-catenin in RSPO2-treated 2-14 cells was examined by immunofluorescence staining **(Fig. 5A-E)**. 2-14 cells cultured in medium containing 2 mM $CaCl_2$ with RSPO2 exhibited nuclear translocation of β-catenin **(Fig. 5C),** while cells

cultured in control medium, with or without $CaCl_2$, did not **(Fig. 5A, B)**. However, additional treatment with DKK1 blocked this translocation in $CaCl_2$- and RSPO2-treated cells **(Fig. 5D)**. No positive reaction was observed in control cells **(Fig. 5E)**.

We furthermore examined active β-catenin by western blotting analysis, because such β-catenin translocate into nuclei[23, 24]. Consequently, we confirmed the increased expression of active β-catenin in $CaCl_2$- and RSPO2-treated cells; we found that it was inhibited by DKK1 treatment **(Fig. 5F, G)**. DKK1 treatment also inhibited RSPO2-induced Alizarin Red S and von Kossa-positive reactions in 2-14 cells **(Fig. 5H, I)**.

4 Discussion

In the present study, we characterized RSPO2 expression in functioning PDL tissue and HPDLCs subjected to stretch loading. In addition, an immature human PDL cell line (2-14 cells) expressed receptors for RSPO2, LGR4; RSPO2 enhanced the osteoblastic differentiation of 2-14 cells through the Wnt/β-catenin signaling pathway. Our results suggest functional roles for RSPO2 in the regulation of osteogenesis in periodontal tissue.

As PDL tissue is continuously subjected to mechanical loading, such as occlusion and mastication, active structural maintenance is required in periodontal tissue[25]. In the current study, we revealed the expression of RSPO2 in rat PDL tissue, and showed its augmentation in stretch-loaded HPDLCs, suggesting the involvement of this protein in PDL tissue function. In particular, as the density of RSPO2 expression in rat PDL tissue was more intense on the bone surface, this protein might contribute to bone formation. Furthermore, the stretch-loading also induced the expression of DKK1, an inhibitor of Wnt/β-catenin signaling. Therefore, the mechanical loading condition might regulate the expression of these proteins. A previous report showed that the integrin-FAK pathway regulates mechanical stress-induced expression of M-CSF, TNF-α, RANKL and OPG[26]; therefore, this pathway may be involved in regulating RSPO2 and DKK1 expressions in PDL tissue.

RSPOs activate the Wnt/β-catenin signaling pathway and act as an important regulator in skeleton development and postnatal bone remodeling[27, 28]. RSPO2 deletion, however, results in the malformation of craniofacial bones, suggesting it plays an important role in the development of these intramembranous bones[29, 30]. Further, RSPO2 knockdown suppressed the enhanced osteoblastic differentiation seen with Wnt11 overexpression[31]. Conversely, over-expression of RSPO2 enhanced the osteoblastic differentiation of MC3T3E1 cells in the presence of BMP. These findings correspond with our data, which revealed enhanced mineralization of immature PDL cells upon RSPO2 treatment. In addition, considering the enhanced expression of DKK1 by stretch loading, mineralization of PDL tissue subjected to mechanical loading may be finely controlled by RSPO2 and DKK1 to prevent PDL tissue from mineralizing excessively.

LGRs, recognized as exquisite markers for self-renewing stem cells, have a high affinity for the furin domains of RSPOs, and have been shown to activate the Wnt/β-catenin signaling pathway[12, 13]. In mice lacking LGR4, bone formation decreased, whereas bone resorption increased[32]. Our study showed the remarkable expression of LGR4, but little of LGR5 and LGR6 in immature human PDL cells, indicating its involvement in RSPO2 signaling. Destabilization of β-catenin was decreased in osteoblasts obtained from OA patients, and recombinant RSPO2 rescued this

destabilization[33]. As our results indicate that RSPO2 increased the expression and nuclear translocation of active β-catenin, RSPO2 might induce osteoblastic differentiation of immature PDL cells via LGR4/β-catenin signaling. Our findings suggest that RSPO2 may play an important role as a positive regulator in the maintenance of periodontal tissue, especially of alveolar bone under mechanical loading, which may be controlled by DKK1 through the Wnt/β-catenin signaling pathway.

Acknowledgements

We thank Drs. Nozu, Itoyama, Ono, Fujino, and Ipposhi for their great support in the preparation of this work. This work was supported by JSPS KAKENHI grant numbers JP15H05023, JP16K20457, JP16K20458, JP17H01598, and JP17H04385.

We thank Ryan Chastain-Gross, Ph.D., from Edanz Group (www.edanzediting.com/ac) for editing a draft of this manuscript.

5 Reference

1. McCulloch CA. Origins and functions of cells essential for periodontal repair: the role of fibroblasts in tissue homeostasis. *Oral Dis* 1995;1:271-278.
2. Bartold PM, McCulloch CA, Narayanan AS, Pitaru S. Tissue engineering: a new paradigm for periodontal regeneration based on molecular and cell biology. *Periodontol 2000* 2000;24:253-269.
3. Shimono M, Ishikawa T, Ishikawa H, et al. Regulatory mechanisms of periodontal regeneration. *Microsc Res Tech* 2003;60:491-502.
4. Henneman S, Bildt MM, Degroot J, Kuijpers-Jagtman AM, Von den Hoff JW. Relaxin stimulates MMP-2 and alpha-smooth muscle actin expression by human periodontal ligament cells. *Arch Oral Biol* 2008;53:161-167.
5. Maeda H, Wada N, Tomokiyo A, Monnouchi S, Akamine A. Prospective potency of TGF-beta1 on maintenance and regeneration of periodontal tissue. *Int Rev Cell Mol Biol* 2013;304:283-367.
6. Beertsen W, McCulloch CA, Sodek J. The periodontal ligament: a unique, multifunctional connective tissue. *Periodontol 2000* 1997;13:20-40.
7. Seo BM, Miura M, Gronthos S, et al. Investigation of multipotent postnatal stem cells from human periodontal ligament. *Lancet* 2004;364:149-155.
8. Fujii S, Maeda H, Wada N, Kano Y, Akamine A. Establishing and characterizing human periodontal ligament fibroblasts immortalized by SV40T-antigen and hTERT gene transfer. *Cell Tissue Res* 2006;324:117-125.
9. Fujii S, Maeda H, Wada N, Tomokiyo A, Saito M, Akamine A. Investigating a clonal human periodontal ligament progenitor/stem cell line in vitro and in vivo. *J Cell Physiol* 2008;215:743-749.
10. Tomokiyo A, Maeda H, Fujii S, Wada N, Shima K, Akamine A. Development of a multipotent clonal human periodontal ligament cell line. *Differentiation* 2008;76:337-347.
11. Nam JS, Turcotte TJ, Smith PF, Choi S, Yoon JK. Mouse cristin/R-spondin family proteins are novel ligands for the Frizzled 8 and LRP6 receptors and activate beta-catenin-dependent gene expression. *J Biol Chem* 2006;281:13247-13257.
12. Carmon KS, Gong X, Lin Q, Thomas A, Liu Q. R-spondins function as ligands of the orphan receptors LGR4 and LGR5 to regulate Wnt/beta-catenin signaling. *Proc Natl Acad Sci U S A* 2011;108:11452-11457.
13. de Lau W, Barker N, Low TY, et al. Lgr5 homologues associate with Wnt receptors and mediate R-spondin signalling. *Nature* 2011;476:293-297.

14. Yamada W, Nagao K, Horikoshi K, et al. Craniofacial malformation in R-spondin2 knockout mice. *Biochem Biophys Res Commun* 2009;381:453-458.
15. Zhu C, Zheng XF, Yang YH, et al. LGR4 acts as a key receptor for R-spondin 2 to promote osteogenesis through Wnt signaling pathway. *Cell Signal* 2016;28:989-1000.
16. Wada N, Maeda H, Tanabe K, et al. Periodontal ligament cells secrete the factor that inhibits osteoclastic differentiation and function: the factor is osteoprotegerin/osteoclastogenesis inhibitory factor. *J Periodontal Res* 2001;36:56-63.
17. Mitarai H, Wada N, Hasegawa D, et al. Transgelin mediates transforming growth factor-beta1-induced proliferation of human periodontal ligament cells. *J Periodontal Res* 2017;52:984-993.
18. Hasegawa D, Wada N, Yoshida S, et al. Wnt5a suppresses osteoblastic differentiation of human periodontal ligament stem cell-like cells via Ror2/JNK signaling. *J Cell Physiol* 2018;233:1752-1762.
19. Hasegawa D, Wada N, Maeda H, et al. Wnt5a Induces Collagen Production by Human Periodontal Ligament Cells Through TGFbeta1-Mediated Upregulation of Periostin Expression. *J Cell Physiol* 2015;230:2647-2660.
20. Fujihara C, Yamada S, Ozaki N, et al. Role of mechanical stress-induced glutamate signaling-associated molecules in cytodifferentiation of periodontal ligament cells. *J Biol Chem* 2010;285:28286-28297.
21. Maeda H, Nakano T, Tomokiyo A, et al. Mineral trioxide aggregate induces bone morphogenetic protein-2 expression and calcification in human periodontal ligament cells. *J Endod* 2010;36:647-652.
22. Wada N, Menicanin D, Shi S, Bartold PM, Gronthos S. Immunomodulatory properties of human periodontal ligament stem cells. *J Cell Physiol* 2009;219:667-676.
23. Kim SE, Huang H, Zhao M, et al. Wnt stabilization of beta-catenin reveals principles for morphogen receptor-scaffold assemblies. *Science* 2013;340:867-870.
24. MacDonald BT, Tamai K, He X. Wnt/beta-catenin signaling: components, mechanisms, and diseases. *Dev Cell* 2009;17:9-26.
25. Monnouchi S, Maeda H, Fujii S, Tomokiyo A, Kono K, Akamine A. The roles of angiotensin II in stretched periodontal ligament cells. *J Dent Res* 2011;90:181-185.
26. Kim SJ, Park KH, Park YG, Lee SW, Kang YG. Compressive stress induced the up-regulation of M-CSF, RANKL, TNF-alpha expression and the down-regulation of OPG expression in PDL cells via the integrin-FAK pathway. *Arch Oral Biol* 2013;58:707-716.
27. Knight MN, Hankenson KD. R-spondins: novel matricellular regulators of the

skeleton. *Matrix Biol* 2014;37:157-161.

28. Shi GX, Mao WW, Zheng XF, Jiang LS. The role of R-spondins and their receptors in bone metabolism. *Prog Biophys Mol Biol* 2016;122:93-100.

29. Nam JS, Turcotte TJ, Yoon JK. Dynamic expression of R-spondin family genes in mouse development. *Gene Expr Patterns* 2007;7:306-312.

30. Hankenson KD, Sweetwyne MT, Shitaye H, Posey KL. Thrombospondins and novel TSR-containing proteins, R-spondins, regulate bone formation and remodeling. *Curr Osteoporos Rep* 2010;8:68-76.

31. Friedman MS, Oyserman SM, Hankenson KD. Wnt11 promotes osteoblast maturation and mineralization through R-spondin 2. *J Biol Chem* 2009;284:14117-14125.

32. Luo J, Zhou W, Zhou X, et al. Regulation of bone formation and remodeling by G-protein-coupled receptor 48. *Development* 2009;136:2747-2756.

33. Abed E, Chan TF, Delalandre A, Martel-Pelletier J, Pelletier JP, Lajeunesse D. R-spondins are newly recognized players in osteoarthritis that regulate Wnt signaling in osteoblasts. *Arthritis Rheum* 2011;63:3865-3875.

Figure

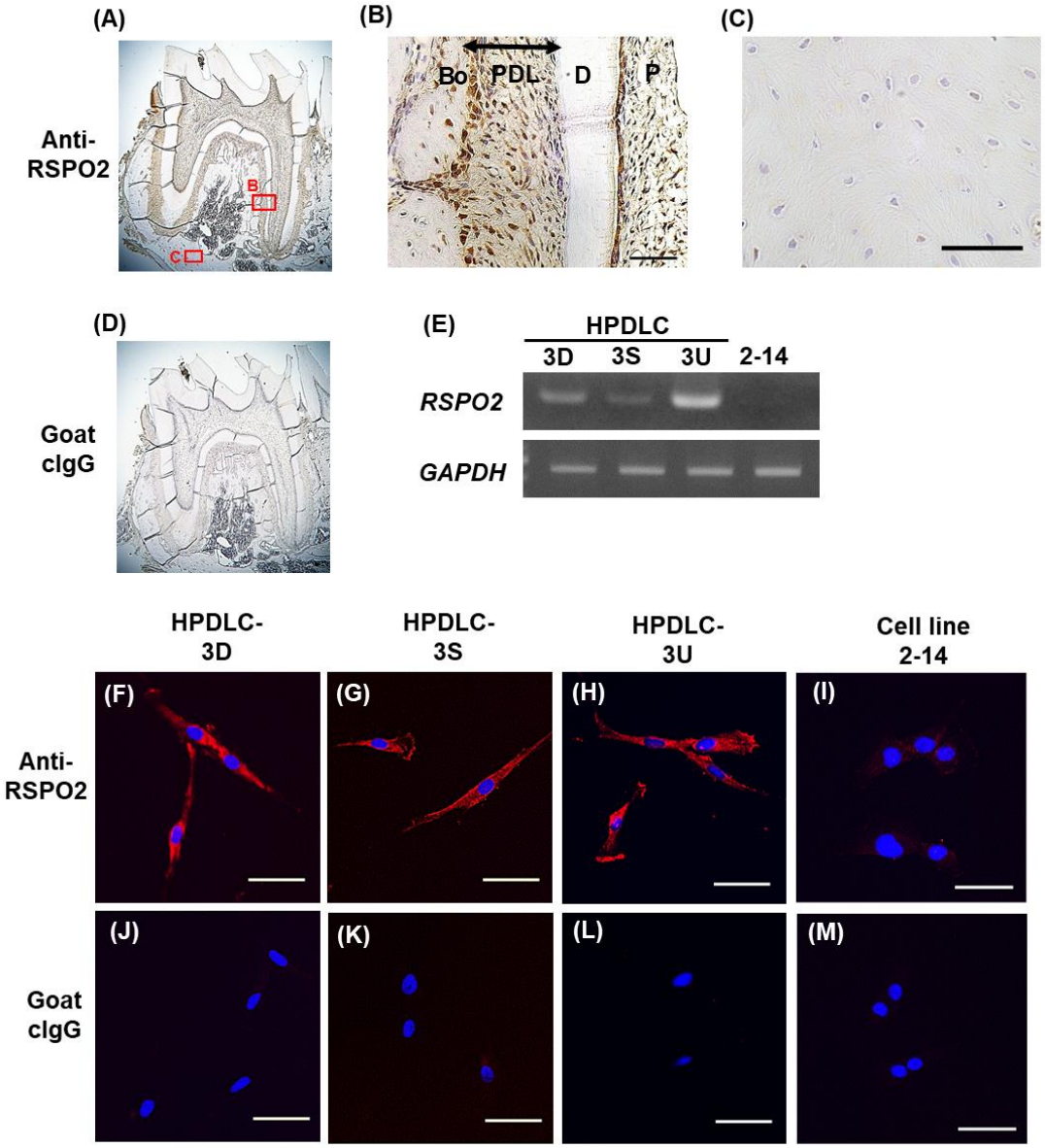

Fig. 1 Expression of RSPO2 in rat PDL tissue, HPDLCs, and 2-14 cells.
(A-C) In the sagittal sections of the lower first molar of 5-week-old male SD rats, immunohistochemical analysis revealed that RSPO2-positive staining was observed throughout the PDL tissue. Nuclei were stained with hematoxylin. Bo, bone; D, dentin; PDL, periodontal ligament; P, pulp. Bars = 200 μm. (B, C) Highly magnified view of boxed areas in A. (D) No positive staining was observed in tissues incubated with goat control IgG (cIgG). (E) The expression of *RSPO2* in HPDLC-3D, HPDLC-3S, HPDLC-3U, and 2-14 cells was examined by semi-quantitative RT-PCR. (F-M) Immunofluorescence staining was positive for RSPO2 in HPDLC-3D (F), HPDLC-3S (G), and HPDLC-3U (H), but faint in 2-14 cells (I). No positive staining was observed in HPDLC-3D (J), HPDLC-3S (K), HPDLC-3U (L), and 2-14 cells (M) treated with goat cIgG. Nuclei were stained with DAPI. Bars = 50 μm.

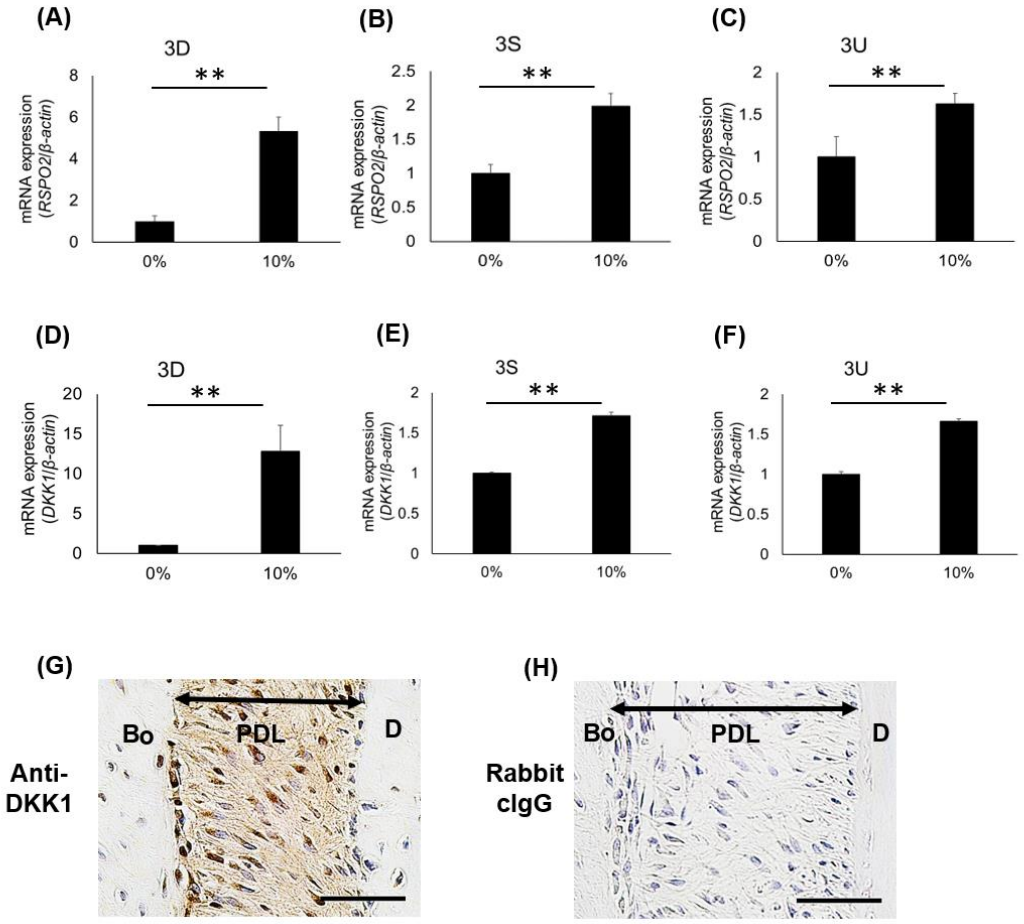

Fig. 2 Effects of stretch loading on *RSPO2* and *DKK1* expression in HPDLCs and expression of DKK1 in rat PDL tissue.
HPDLC-3D (A, D), HPDLC-3S (B, E), and HPDLC-3U (C, F) cultures were exposed to stretch loading of 10% (0.5 Hz) elongation for 24 hours, and *RSPO2* (A-C) and *DKK1* (D-F) expression in each cell culture was assessed by quantitative RT-PCR. All values are ratios relative to 0% elongation. All values are means ± SD of quadruplicate assays. **P<0.01, vs 0% elongation. (G) Immunohistochemical analysis revealed that DKK1-positive staining was observed throughout the PDL tissue. Nuclei were stained with hematoxylin. Bo, bone; D, dentin; PDL, periodontal ligament. Bars = 200 μm. (H) No positive staining was observed in tissues incubated with rabbit control IgG (cIgG).

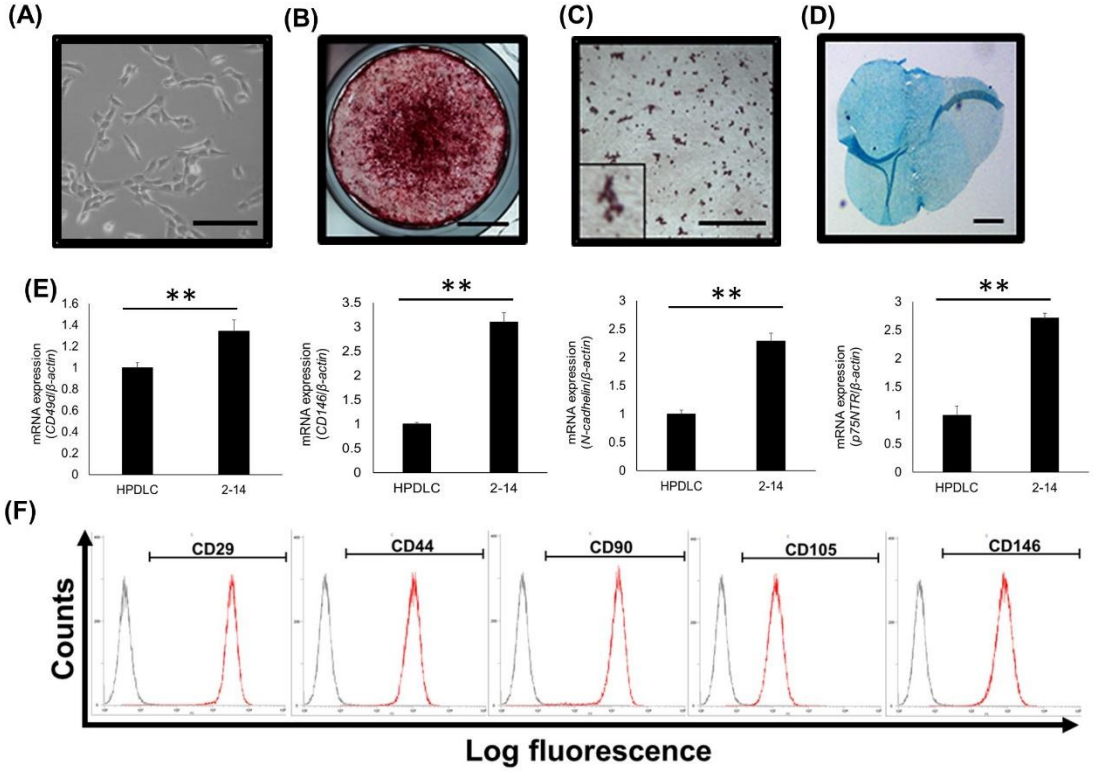

Fig. 3 The characterization of 2-14 cells.
(A) Phase-contrast view of 2-14 cells. Bars = 200 μm. (B-D) The differentiation potential of 2-14 cells. (B) Alizarin Red S staining of 2-14 cells cultured in osteoblastic differentiation medium for 2 weeks. Bars = 5 mm. (C) Oil Red O staining of 2-14 cells cultured in adipogenic inductive condition for 3 weeks. Inset, higher magnified view of Oil Red O-positive lipid. Bars = 20 μm. (D) Alcian blue staining of 2-14 cells cultured in chondrogenic inductive condition for 4 weeks. Bars = 200 μm. (E) The expression of stem cell markers (*CD49d, CD146, N-cadhelin,* and *p75NTR*) in 2-14 cells was assessed by quantitative RT-PCR. All values are ratios relative to HPDLCs. All values are means ± SD of quadruplicate assays. **P<0.01, vs HPDLCs. (F) Flow cytometric analysis demonstrated the intensities of CD29, CD44, CD90, CD105, and CD146 expression in 2-14 cells (red line).

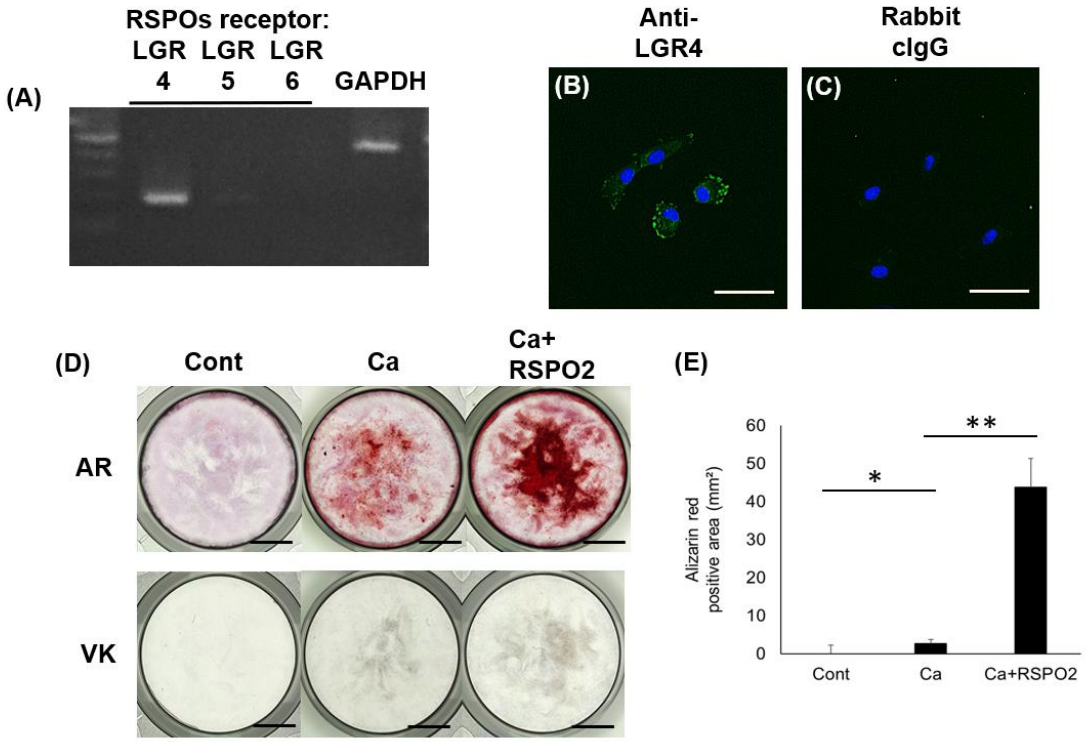

Fig. 4 Expression of receptors of RSPO2 in 2-14 cells and the effects of RSPO2 on the osteoblastic differentiation of 2-14 cells.
(A) The mRNA expression of receptors of RSPO (*LGR4, LGR5, and LGR6*) in 2-14 cells was examined by semi-quantitative RT-PCR. (B) Immunofluorescence staining exhibited positive staining for LGR4 in 2-14 cells. (C) No positive staining was observed in 2-14 cells treated with goat control IgG (cIgG). Nuclei were stained with DAPI. Bars = 50 μm. (D) Alizarin Red S (AR) and von Kossa (VK) stainings of 2-14 cells cultured in osteoblastic differentiation medium, with or without 100 ng/ml RSPO2 for 20 days. Bars = 5 mm. (E) The graph shows the quantitative analysis of the area of Alizarin Red-positive region, which was imaged and measured using a Biozero digital microscope (Keyence).

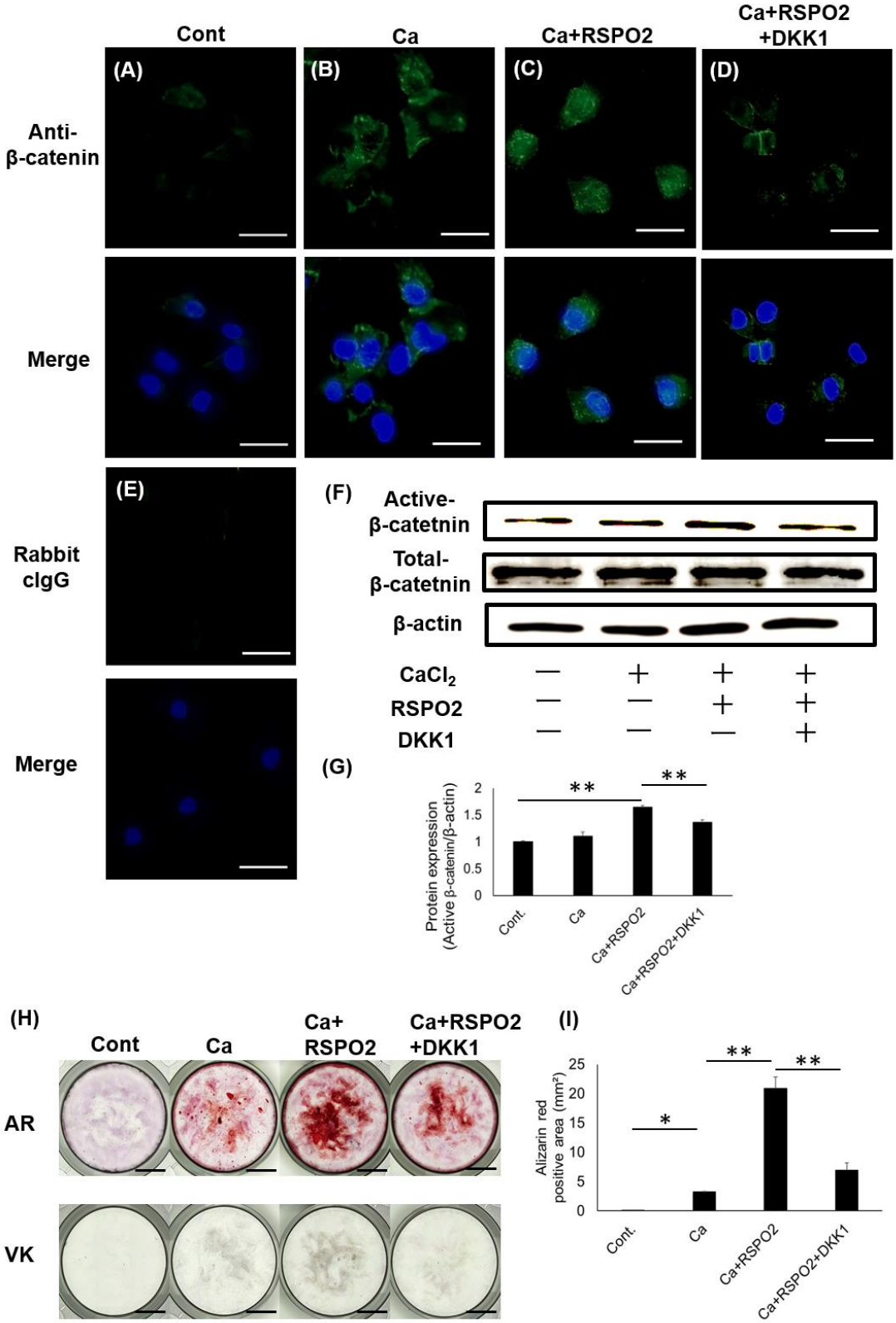
Cont
Ca
Ca+RSPO2
Ca+RSPO2
+DKK1
(A)
(B)
(C)
(D)
Anti-
β-catenin
Merge
(E)
Rabbit
cIgG
Merge
(F)
Active-
β-catetnin
Total-
β-catetnin
β-actin
CaCl2
RSPO2
DKK1
(G)
Protein expression
(Active β-catenin/β-actin)
Cont.
Ca
Ca+RSPO2
Ca+RSPO2+DKK1
(H)
Cont
Ca
Ca+
RSPO2
Ca+RSPO2
+DKK1
AR
VK
(I)
Alizarin red
positive area (mm²)
Cont.
Ca
Ca+RSPO2
Ca+RSPO2+DKK1

Fig. 5 Involvement of Wnt/β-catenin signaling pathway in RSPO2-induced osteoblastic differentiation of 2-14 cells.
Immunofluorescence staining elucidated localization of β-catenin in 2-14 cells. 2-14 cells cultured in control medium (Cont) (A); with 2 mM $CaCl_2$ (Ca) (B); with 2 mM $CaCl_2$ and 100 ng/ml RSPO2 (Ca+RSPO2) (C); and with 2 mM $CaCl_2$, 100 ng/ml RSPO2, and 100 ng/ml DKK1 (Ca+RSPO2+DKK1) (D). No positive staining was observed in 2-14 cells treated with rabbit control IgG (cIgG) (E). Nuclei were stained with DAPI. Bars = 50 μm. (F) β-catenin and active β-catenin expression were determined by western blotting analysis. (G) The graph shows the quantitative analysis of active β-catenin based on western blotting analysis data. Data are shown as the means ± SD of triplicate samples from representative experiments. **$P<0.01$. (H) Alizarin Red S (AR) and von Kossa (VK) stainings of 2-14 cells cultured in control medium (Cont) or osteoblastic differentiation medium (Ca), with or without 100 ng/ml RSPO2, in the presence or absence of 100 ng/ml DKK1 for 20 days. Bars = 5 mm. (I) The graph shows the quantitative analysis of the area of Alizarin Red-positive region, which was imaged and measured using a Biozero digital microscope (Keyence).

Table 1. Primer sequence, product size, annealing temperature, for semi-quantitative RT-PCR

Target gene (abbreviation)	Gene Bank ID	Forward (top) and reverse(bottom) primer sequences	Cycles	Size of amplified Products (bp)	Annealing Temperature (°C)
R-spondin2	NM_178565.4	5'-CTGTGTCCAACCATTGCTGA-3'	35	150	56
		5'-GAAGACGCTGTGTTGCTCCT-3'			
LGR4	NM_18490.3	5'-AGAAGAGCTACAATTGGCGG-3'	30	193	57
		5'-GTCCTCGGGGACTGAGGTAA-3'			
LGR5	NM_003667.3	5'-CCCACACACTGTCATTGCGA-3'	30	193	58
		5'-CCGCAAGACGTAACTCCTCC-3'			
LGR6	NM_001017404.1	5'-TCACACATCCCAGGACAAGC-3'	30	133	56
		5'-AATTCAGGTCTAGCGACTGC-3'			
GAPDH	NM_001256799.2	5'-ACCACAGTCCATGCCATCCAC-3'	18	452	60
		5'-TCCACCACCCTGTTGCTGTA-3'			

Table 2. Primer sequence, product size, annealing temperature, for quantitative RT-PCR

Target gene (abbreviation)	Gene Bank ID	Forward (top) and reverse(bottom) primer sequences	Size of amplified Products (bp)	Annealing Temperature (°C)
DKK1	NM_012242.3	5'-GCACCTTGGATGGGTATTCCA-3'	181	60
		5'-TGCTTGGTACACACTTGACCT-3'		
R-spondin2	NM_178565.4	5'-CTGTGTCCAACCATTGCTGA-3'	150	60
		5'-GAAGACGCTGTGTTGCTCCT-3'		
CD49d	NM_000885.5	5'-AAGGCCGGCCATCCATTTTAGAAA-3'	142	60
		5'-AGTCCTTCCAGTAGAACATGCGCA-3'		
CD146	NM_006500.2	5'-GGCTGTGATTGTGTGCATCC-3'	134	60
		5'-GTTCGCTCTTACGAGACGGG-3'		
N-cadhelin	NM_001792.4	5'-GAAAGACCCATCCACGCCGAGC-3'	101	60
		5'-TCAGCCGCTTTAAGGCCCTCATT-3'		
p75NTR	NM_002507.3	5'-CCGAGGCACCACCGACAACC-3'	108	60
		5'-TGCTTGCAGCTGTTCCACCTCT-3'		
β-actin	NM_001101.3	5'-ATTGCCGACAGGATGCAGA-3'	89	60
		5'-GAGTACTTGCGCTCAGGAGGA-3'		